A PASSIVE HUMIDITY MONITORING SYSTEM FOR IN-SITU REMOTE WIRELESS TESTING OF MICROPACKAGES

T. Harpster, S. Hauvespre, M. Dokmeci, B. Stark, A. Vosoughi, and K. Najafi
Center For Integrated Microsystems
University of Michigan, Ann Arbor MI 48109-2122

ABSTRACT

This paper reports a small passive wireless humidity monitoring system (HMS) for continuous monitoring of humidity changes inside miniature hermetic packages, presents its application in determining hermeticity of an implantable biomedical package, and presents long-term performance results obtained from packages implanted in guinea pigs. This $7\times1.2\times1.5mm^3$ system consists of a high-sensitivity capacitive humidity sensor that forms an LC tank circuit together with a hybrid coil wound around a ferrite substrate. The resonant frequency of the circuit changes when the humidity sensor capacitance changes in response to changes in humidity. The HMS can resolve humidity changes of ±2.5%RH over a 2cm range. The resolution is sufficient enough to monitor internal package humidity for either in in-vitro or in-vivo testing.

INTRODUCTION

In the past few years, much attention has been focused on the development of miniature hermetic packages for protection of MEMS and integrated circuitry from harsh external environments in many applications. To assess the suitability of a particular package for a specific application, different testing techniques have been developed to determine mean-time-to-failure by creating an accelerated test condition. Although accelerated testing is very important and useful, many emerging applications require the package to be tested in its real world environment, or be continuously monitored in-situ. For example, in implantable biomedical applications, in-vivo testing of the package hermeticity is necessary since it is not possible to accurately reproduce biological conditions in-vitro [1]. Furthermore, many packages developed for microsystems are small with a sealed cavity of no more than a few mm^3 in volume. Therefore, miniature monitoring systems that can be used for long-term package testing in-situ are needed.

A miniature implantable hermetic package with multiple feedthroughs using glass-silicon anodic bonding technology has been developed for biomedical applications [1]. One specific application of this implantable package has been used for a neuromuscular stimulator. The hermetic glass-silicon package provides protection for integrated circuitry and hybrid components. Accelerated testing results for the glass-silicon package indicate a mean-time-to-failure of several decades in saline at 37°C [2]. Dew point sensors were incorporated into the package and used to compile this lifetime data. Dew point sensors merely indicate when the package admits moisture into the sealed cavity, and does not provide any information about changes in relative humidity inside the package which would be useful in detecting the onset of failure. Also, the dew point sensors had to be physically probed, via the feedthroughs, and thus could not be used for testing in-vivo.

An improved sensor for monitoring package hermeticity should incorporate a high-sensitivity humidity sensor and telemetric circuitry for wireless humidity monitoring. Active circuitry complicates the fabrication process; therefore, a passive telemetric circuit is preferred.

DESIGN AND ANALYSIS

Figure 1 depicts a passive humidity monitoring system for use in this and other applications. This system consists of a miniature high-sensitivity capacitive humidity sensor [3] and a hybrid coil wound around a ferrite substrate forming an LC tank circuit. The resonant frequency of the circuit is determined by the humidity sensor capacitance, which changes in response to humidity. To remotely monitor the resonant frequency shift, a circular loop antenna is used to stimulate the tank circuit.

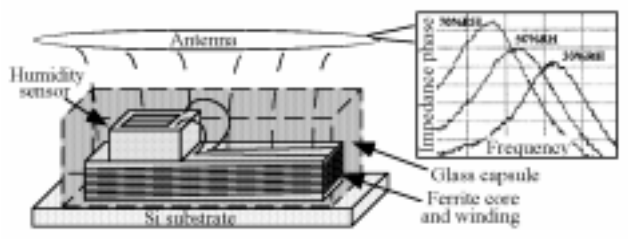

Figure 1: Passive humidity monitoring system.

This resonant frequency shift, also shown in Figure 1, is measured as a change in the load impedance reflected back to the antenna, as illustrated in the equivalent circuit shown in Figure 2. It will be shown that the reflected load impedance is a function of the humidity sensor capacitance. As this reflected load changes, the overall

impedance of the transmitter antenna changes, thus one can extract the resonant frequency by monitoring the impedance change of the transmitting antenna.

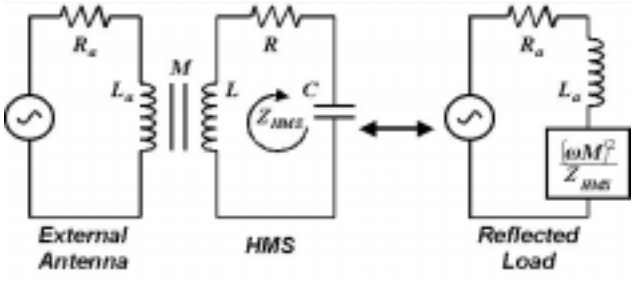

Figure 2: HMS equivalent circuit model.

The equivalent circuit is used to model the HMS and aid in optimizing the sensor performance. The following assumptions are made to simplify the inductive coupling of the equivalent circuit model: 1) the antenna and HMS coils are aligned coaxially; and 2) the HMS cross sectional area is much smaller than the external antenna. These assumptions allow the following approximations to be made: 1) the magnetic field of the external antenna will be calculated only along the coaxial z-axis, thus the magnetic field is a function $B(z)$; and 2) the magnetic field being coupled to the HMS will be assumed constant across the HMS cross section. Equation nomenclature is given in Table 1.

Table 1: Circuit model equation nomenclature.

Antenna:		Humidity sensing system:	
L_a	inductance	C	HS capacitance
r_a	radius	R	series resistance
N_a	number of turns	L	coil inductance
R_a	series resistance	N	number of turns
μ_a	core permeability	S	cross sectional area
		μ	core permeability
Coupling:		h	coil height
M	mutual inductance	k	empirical constant [5]

Using Biot-Savart's law for a circular loop with radius r_a, number of windings N_a, carrying current I_a, the calculated magnetic flux density through external antenna along the z-axis is at a distance z given by:

$$B(z) = \mu_a H(z) = \frac{\mu_a N_a I_a r_a^2}{2(r_a^2 + z^2)^{3/2}} \left[\frac{Wb}{m^2}\right] \qquad \text{(Eq. 1)}$$

The antenna inductance is

$$L_a = \frac{\mu_a \pi N_a^2 r_a}{2} [H] \qquad \text{(Eq. 2)}$$

The mutual inductance, a ratio of flux linkage on the HMS circuit due to the current in the external antenna, is calculated as

$$M(z) = \frac{\mu N}{\mu_o I_a} \int_S B \cdot dS = \frac{\mu \mu_a r_a^2 N_a N S}{2\mu_o (r_a^2 + z^2)^{3/2}} [\mathrm{H}] \qquad \text{(Eq. 3)}$$

The inductance, L_o, of a finite length solenoid is used to approximate the HMS coil [5].

$$L_o = k \frac{\mu N^2 \pi r_o^2}{l_o} [\mathrm{H}] \qquad \text{(Eq. 4)}$$

where r_o is the radius of the solenoid, l_o is the solenoid length, and the dimensionless factor, k, is a function of the ratio l_o/r_o. The following approximations are made to correlate the HMS inductance, L, with the finite solenoid expression: the cross sectional area of the HMS coil, S = 7mm^2, is equal to the cross sectional area of the solenoid, πr_o^2; also the height of the HMS coil, h = 1mm, is equal to the length of the solenoid, l_o. The dimensionless factor, k, is obtained [5] and thus the final expression for the HMS inductance, L, is

$$L = 0.45 \frac{\mu N^2 S}{h} [\mathrm{H}] \qquad \text{(Eq. 5)}$$

The impedance of the HMS is

$$Z_{HMS}(\omega) = R + j\left(\omega L - \frac{1}{\omega C}\right) \qquad \text{(Eq. 6)}$$

The impedance seen at the external antenna is given by

$$Z(\omega) = R_a + j\,\omega L_a + \frac{\omega^2 M^2}{Z_{HMS}(\omega)} \qquad \text{(Eq. 7)}$$

From Eqs. 6 & 7, at the resonance frequency of the HMS circuit the impedance of the external antenna is

$$Z(\omega_o) = R_a + j\,L_a\omega_o + \frac{\omega_o^2 M^2}{R} \qquad \text{(Eq. 8)}$$

For maximum reflected impedance the last term of Eq. 8 is maximized and the imaginary part is minimized. This is accomplished by increasing μ, μ_a, N, and S and decreasing r_a, z, and N_a. Figure 3 shows $|Z(\omega)|$ and $\angle Z(\omega)$ for decreasing separation distance, z = 1, 0.5 and 0cm, as seen in the increase in phase dip. Note that

increasing μ, μ_a, N, and S and decreasing r_a, z, and N_a produces the same effect. Also, note that decreasing R will increase the Q of the resonant circuit as well as increase the reflected impedance and thus increase the phase dip.

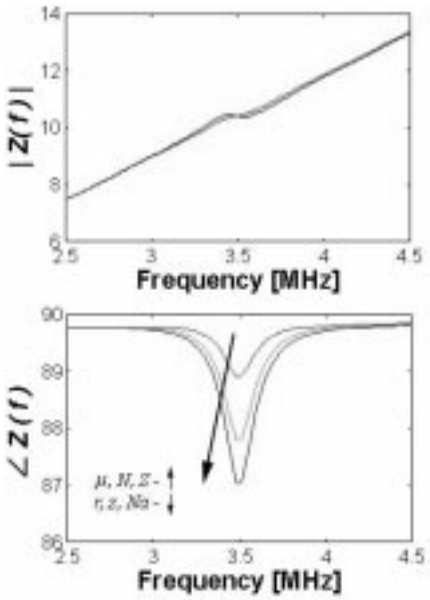

Figure 3: Simulation of antenna impedance, Z(*f*).

Maximum reflected impedance is desired for resonant frequency measurement and increased maximum testing distance; however, only the HMS resonant frequency, ω_o, is needed for humidity monitoring, which is independent of the reflected impedance magnitude and is identified at the phase minima.

FABRICATION

An SEM photograph of the complete 7×1.2×1.5mm^3 system is shown in Figure 4.

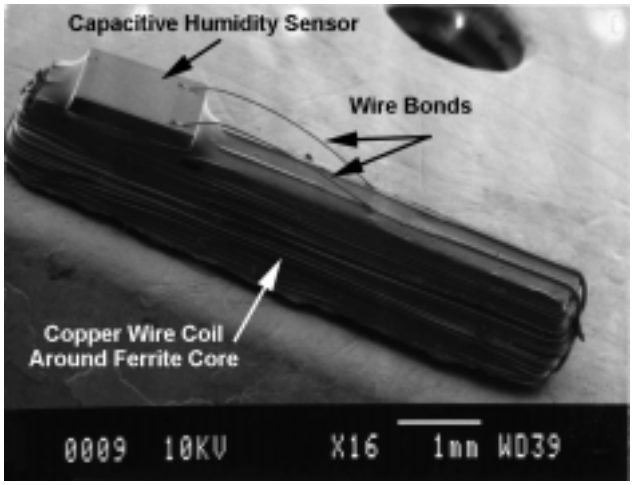

Figure 4: SEM of a fabricated HMS.

For high sensitivity, a polyimide humidity sensor (1×1×.5mm^3) [3], whose capacitance varies from 180-240pF for 20-80%RH change, is used. This sensor is wire bonded to a hybrid copper wire coil forming an LC tank circuit. The coil is constructed by winding ≅25 turns of 44awg copper wire around a NiFe ferrite core. The entire structure is assembled using PI2611 polyimide as an epoxy. The impedance of the external stimulating loop antenna, (24awg tin wire, 4-8 turns, ≅1.5-2cm diameter), is measured with high resolution using an HP4194A Impedance/Gain-Phase Analyzer. Experimental values for R_a, L_a, R, L and C are listed in Table 2.

Table 2: Experimental values

R_a	–	200 mΩ
L_a	–	400 nH
R	–	15–20 Ω
L	–	6–20 μH
C	–	180–240 pF

These values are sufficiently modeled with the described theory; however, for exact values, the relative permeability must be derived for the HMS ferrite core.

RESOLUTION AND SENSITIVITY

Figure 5 shows the measured $|Z(\omega)|$ and $\angle Z(\omega)$ of a fabricated system.

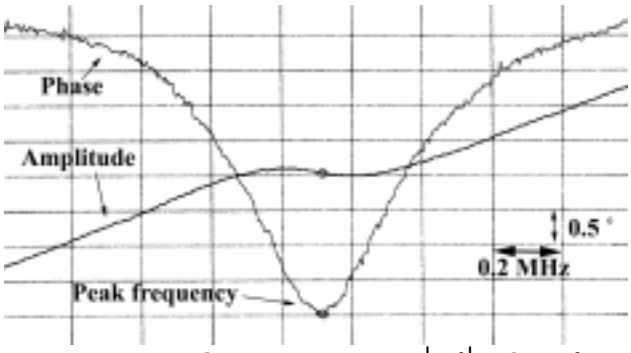

Figure 5: Impedance measurements $|Z(f)|$ and $\angle Z(f)$.

An HMS is placed on a hot plate at 350°C to drive all residual moisture out of the humidity sensor. The HMS is then placed in an ESPEC temperature and humidity chamber to calibrate the device. The temperature of the chamber is set to 37°C and the impedance of a loop antenna (coupled to the hybrid coil-humidity sensor inside the chamber) is measured to monitor the HMS resonant frequency as humidity is controlled from 20% to 80% RH at 10% intervals. The results are shown in Figure 6.

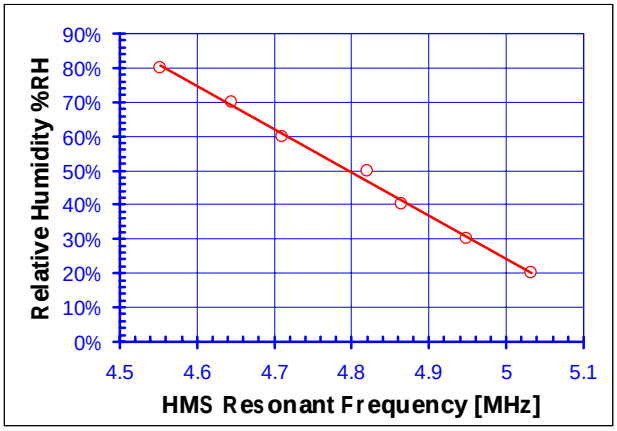

Figure 6: HMS calibration curve.

The sensitivity of the system is extracted from the slope of the calibration curve and is about 8kHz/%RH for this specific sensor. Other HMSs have been calibrated with sensitivities ranging from 5-8kHz/%RH. The resonant frequency measurement is ±12.5kHz, giving the overall wireless system a resolution ±2.5%RH.

Using a ferrite material in the antenna core allows the permeability μ_a to be increased by a factor μ_r (μ_r is determined by the ferrite material characteristics). From Eqs. 2, 3, & 8, the real part to imaginary part of $Z(\omega_o)$ is increased by μ_r thus the sensitivity of the system is increased. Figure 7 shows the response of an antenna with a ferrite (material #61) core and with an air core.

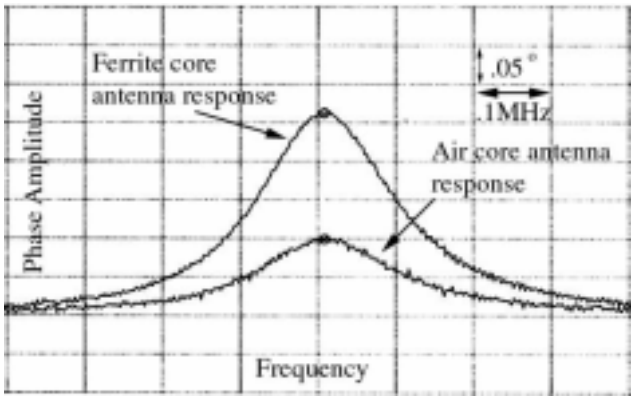

Figure 7: Phase amplitude of ferrite core and non-ferrite core loop antenna.

Both the measurement distance, and the sensitivity can be improved by using a ferrite core in the transmitting antenna; however, ferrite core antennas can only be used to test the HMS for a given range due to an observable resonant frequency shift at close distances, shown in Figure 8.

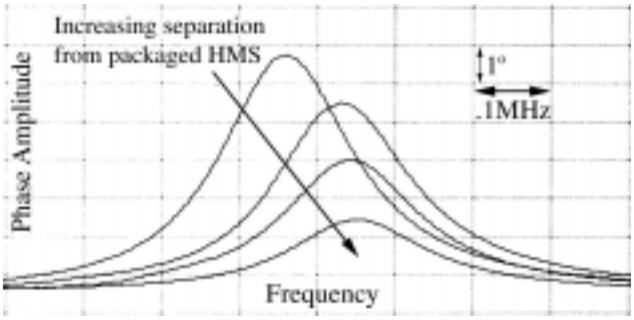

Figure 8: Observed frequency shift only with ferrite core antenna.

This frequency shift is attributed to the increased magnetic field of the ferrite core antenna on the HMS ferrite core inductor coil. The permeability of a ferrite material is nonlinearly proportional to the magnetic flux density impressed upon it. Therefore, as the antenna moves closer to the HMS the magnetic flux density in the HMS ferrite core increases. This increases the permeability of the HMS ferrite and thereby increases the coil inductance. Note the resonant frequency of the HMS is

$$f_o = \frac{1}{2\pi\sqrt{LC}}[\text{Hz}] \qquad \text{(Eq. 9)}$$

thus a decrease in resonant frequency is observed when the ferrite antenna is close to the HMS. Figure 9 shows an acceptable range of 0.2-2cm for using a ferrite antenna.

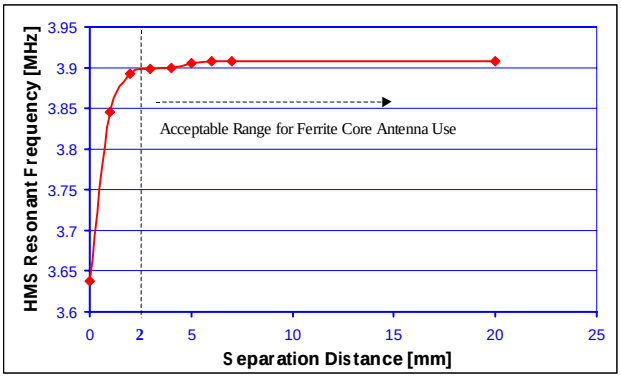

Figure 9: Testing range of ferrite core antenna.

This is an improvement because air core antennas are only useful up to 1cm from the HMS. Increased antenna sensitivity with ferrite core antennas allows extended testing distances, which may be useful for animal implant testing. Both of these testing ranges are sufficient for many applications.

TEST RESULTS

The HMS has been utilized in the previously described implantable hermetic glass-silicon package [1]. A packaged HMS, shown in Figure 10, has been tested in-vitro under both accelerated and standard conditions, and tested in-vivo implanted in several guinea pigs.

Figure 10: Glass-silicon package with HMS enclosed.

HMS In-Vitro Test Results

An HMS is encapsulated in a glass-silicon package which has an unbonded region of ≅5mm (due to particle contamination on the bond region). The unbonded region is visually detected using a microscope focused through the glass capsule onto the glass-silicon bond interface. This package is placed into a controllable humidity chamber and the HMS is telemetrically monitored to test the response of the HMS within the non-hermetically sealed package. The HMS data is provided in Figure 11.

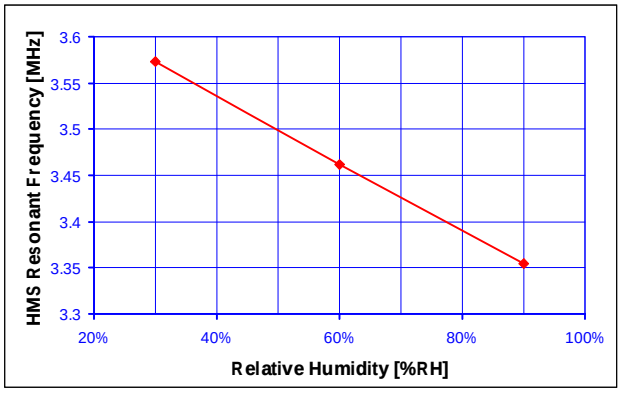

Figure 11: HMS data within a non-hermetic package

In this case, the leakage path is large thus the humidity within the package is immediately affected by the humidity in the external environment as seen by a change in resonant frequency. Thus, gross leakage is detected.

Another HMS is encapsulated in a second glass-silicon package in a dry environment. The package is immersed in DI water at room temperature and monitored visually and telemetrically. While non-hermeticity of the package cannot be confirmed visually, RH monitoring identified this package seal to be non-hermetic. Figure 12 shows the %RH change over a period of 80 days and shows a leakage rate with an indicated exponential humidity increase over the first 3 day soak period and a linear humidity increase for the remaining soak period. Note that the humidity sensor is not linearly characterized for RH<20% thus the nonlinearity may be characteristic of the HS [3].

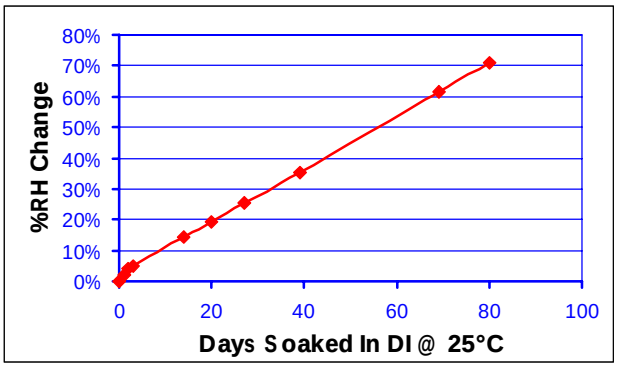

Figure 12: Packaged HMS detecting low leak rate.

In this case, the leakage path is small thus the humidity within the package slowly increases over time and an extremely low leakage rate is detected.

In-vitro test results on a single hermetically sealed package immersed in saline solution at 97°C show no appreciable change in humidity inside the package. The results shown in Figure 13 show the %RH change versus the number of days soaking at 97°C.

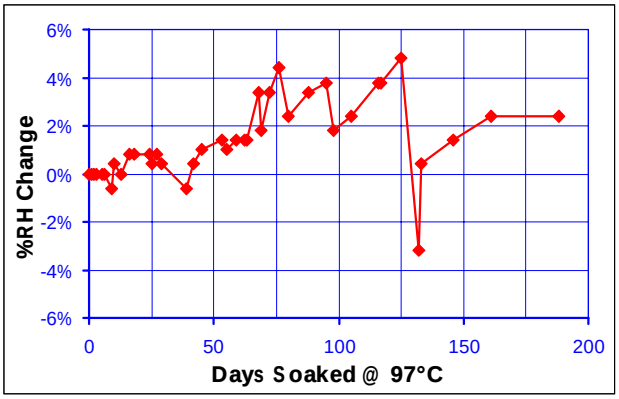

Figure 13: In-vitro test in saline solution at 97°C.

The package is removed from the high temperature environment and brought to room temperature for wireless humidity monitoring. The frequency variations are attributed to thermal shock and day to day temperature fluctuations during testing since relative humidity is temperature dependent. These variations are within experimental error and hence the HMS data and visual inspection analysis strongly suggest the anodically sealed package is hermetic.

These in-vitro tests conclusively demonstrate that the HMS can be used to accurately detect non-hermeticity of a fabricated package.

HMS In-Vivo Test Results

With the development of the wireless humidity monitoring system, it is possible to remotely monitor package integrity while the device is implanted in animal hosts. Two guinea pigs have each been implanted with three packages for in-vivo monitoring. Devices were implanted in the head beneath the skull above the dura, under the skin over the leg muscles, and in the abdominal cavity. One of the guinea pigs is shown in Figure 14.

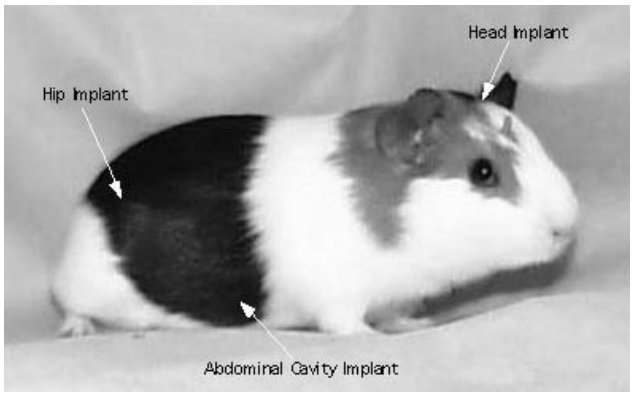

Figure 14: Implanted packages in a guinea pig host.

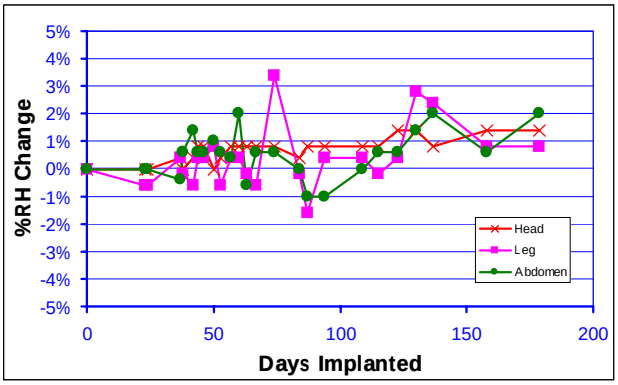

Figure 15: %RH change for three animal implants.

Implanted packages in guinea pigs are monitored bi-weekly and the humidity inside the package is recorded. Figure 15 shows the resonant frequency of three packages in one of the guinea pigs. The resonant frequency has not significantly changed since its initial value at dry conditions, which indicates that the enclosed HMS is dry after 6 months.

CONCLUSION

A miniature humidity monitoring system has been developed for use in implantable biomedical packages. The system can be used to detect humidity changes within ±2.5%RH up to 2cm from a stimulating external ferrite core loop antenna. A simple circuit model has been analyzed which sufficiently models the wireless humidity monitoring system. HMSs have been encapsulated in glass-silicon packages for in-vitro and in-vivo tests.

Future work will implement this wireless monitoring system into a fully automated test station, another useful application for this technology. Also, research will be focused on scaling and eventually integrating the receiver coil on the sensor chip to develop a fully integrated humidity monitoring system.

ACKNOWLEDGEMENTS

The authors wish to thank Dr. F. T. Hambrecht and Dr. W. J. Heetderks of the National Institute of Health for their guidance and encouragement. This research is supported by the NIH, under contract # NIH-N01-NS-8-2387.

REFERENCES

[1] B.Ziaie, J. Von Arx, M. Dokmeci and K. Najafi, "A Hermetic Glass Silicon Micropackage with High-Density On-Chip Feedthroughs for Sensors and Actuators." JMEMS, pp.166-179, Vol. 5, No. 3, Sept. 1996.

[2] M. Dokmeci, J. Von Arx and K. Najafi. "Accelerated Testing of Anodically Bonded Glass-Silicon Packages in Salt Water", *Proc. 9th. Int. Conf. Solid State Sensors & Actuators*, pp. 283-86, June 1997.

[3] M. Dokmeci and K. Najafi, "A High Sensitivity Polyimide Humidity Sensor for Monitoring Hermetic Micropackages." MEMS'99, pp. 279-284, Jan. 1999

[4] Sadiku, Matthew N. O., Elements of Electromagnetics. New York, Oxford University Press, 1995.

[5] Donald G. Fink & H. Wayne Beaty. Standard Hanbook for Electrical Engineers. 13th ed. McGraw-Hill Inc. 1993.